T. C. Ku
J. H. Ramsey
W. C. Clinton

Calculation of Liquid Droplet Profiles from Closed-Form Solution of Young-Laplace Equation

Abstract: A closed-form solution is obtained for a two-dimensional version of the Young-Laplace equation governing the shape of the interface between immiscible liquids. This solution enables designers of liquid junctions (in, for example, soldering or ink printing applications) to calculate profiles using certain junction dimensions as boundary conditions in the equations. Calculated profiles are superimposed on silhouettes of liquid junctions to show the accuracy of the solutions ($\pm 5\%$). The paper also introduces a parameter called the coefficient of retardation which was found convenient in accounting for all the factors that permit variable contact angles to be observed in a given solid-liquid-air system.

Introduction

This paper is concerned with the cross-sectional shapes assumed by small amounts of liquids when they are deposited on a surface. From a practical standpoint, the liquids of interest are solder and printing inks. In the case of solder, the cross-sectional shape, or profile, of the junction can have a significant effect on the electrical and mechanical properties of the devices joined together. Hence, people who wish to assure good junctions conventionally experiment with different solder compositions at various temperatures until they arrive at the combination that produces the desired junction profile.

Similarly, the profile of ink deposited during the printing process has a considerable effect on the features of the printed characters. In this case, the common practice is to try different inks, papers, printing rates, etc. until satisfactory printing is achieved.

The present study is motivated by a desire to eliminate some of the trial-and-error procedures presently used to obtain high quality soldering and printing. The approach used is to postulate an analytical model whereby certain easily measurable properties of a liquid and the surface on which it is to be deposited can be used to predict the dimensions of the liquid profile. For this model the profile is viewed as a thin sheet of liquid attached to the edge of a half-plane. Although such a model represents a considerable compromise with reality, the relative ease of computation and the excellent agreement between calculated and observed profiles makes it useful for the purpose intended.

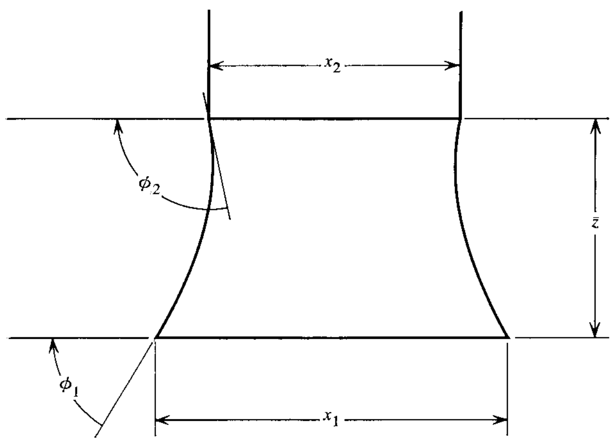

Figure 1 Geometry of liquid junction.

The mathematical form of the model is primarily based on classical surface physics. To account for the fact that the contact angle actually measured in a given system can vary widely between the limits of the advancing and receding contact angles, an empirical factor called the coefficient of retardation is introduced.

The problem

A design problem typical of those to which this paper is addressed is illustrated in Fig. 1. A liquid (ink or solder) junction is shown and it is assumed that the widths of the top and bottom of the junction are specified, as is the height of the junction. The designer may wish to specify further

Authors are at the Systems Development Division Laboratory in Endicott, N.Y.

the angles that the liquid makes with the top and bottom surfaces. With this information he needs to determine analytically the profile of the joint, the area of the profile (which corresponds to the amount of liquid that must be used) and an appropriate liquid material.

The approach to be used in solving this problem is outlined as follows. Any liquid may be characterized for the purpose intended here by constants that can be obtained from some easily made measurements. If a drop of liquid is placed on a surface, measurement of the height of the drop, the width of its base, and the area of the profile are sufficient to provide the characteristic constants. With a knowledge of these constants, it becomes a straightforward matter to calculate the profiles that will occur when this liquid is subjected to other constraints on its geometry.

Some further experiments on the liquid will reveal the limits on the values of contact angles (ϕ_1 and ϕ_2 in Fig. 1) that may be specified by the designer. First, liquid is added to the drop until the contact angle reaches a critical value, at which time the base of the liquid will spread; this angle is called the "advancing angle." Similarly, liquid is removed from the drop until a critical, "receding angle" is reached, such that the base of the liquid will contract. These two angles define the limits on the contact angle for a given liquid-solid connection.

In the following section the equations for characterizing liquids are derived. Subsequent sections present the equations for computing the profiles under a variety of geometric constraints, and an experimental verification of the analysis.

Characterization of liquids

• *The liquid constant*

If two immiscible liquids, a and b, are in equilibrium, and if they are separated by an interface, the shape of the interface is governed by the Young-Laplace equation[1]

$$\frac{1}{R_1} + \frac{1}{R_2} = \frac{1}{\gamma_{ab}} (P_b - P_a) , \tag{1}$$

where R_1 and R_2 are the principal radii of curvature at a given point on the interface, $P_b - P_a$ is the pressure differential across the interface, and γ_{ab} is the interfacial tension. Bashforth and Adams[2] used this equation in 1883 for determining the relationship of an axially symmetric, sessile drop to the surface tension of the liquid and the contact angle it makes with the solid. The case for the axially symmetric hanging drop was treated by Andreas, Hauser, and Tucker.[3] Goldmann has recently used this model to compute the axial symmetrical shape of a solder junction with a numerical approach.[4] In this paper we are concerned with two-dimensional profiles, for which it becomes possible to derive a closed-form analytical solution. These profiles are treated as cross sections of infinitely long bars, rather than as cross sections of axially symmetric drops.

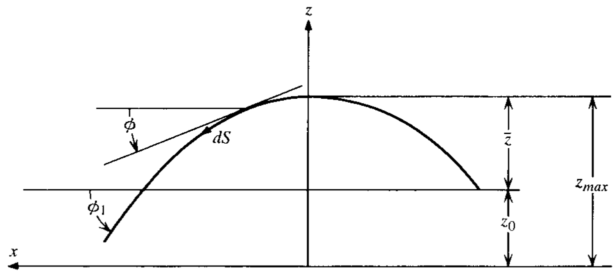

Figure 2 Dimensions used for calculating profile of droplet on surface.

When the pressure is due entirely to the gravitational force, as in a liquid-air interface, and R_2 of Eq. (1) is set equal to infinity, the equation can be written with sufficient accuracy as

$$\frac{d\phi}{dS} = \frac{1}{\gamma_{al}} (P_l - P_a) = \frac{g(\rho_l - \rho_a)}{\gamma_{al}} Z = cZ , \tag{2}$$

where ϕ is the angle made by the tangent to the liquid-air interface and the x axis, S is the distance along the surface, γ_{al} is the surface tension of the liquid, g is the gravitational acceleration, P_l and P_a are the pressures, and ρ_l and ρ_a are the densities of the liquid and air, respectively. The distance Z is to be measured vertically from a horizontal plane ($Z = 0$) at which $P_l - P_a = 0$; i.e., at which $d\phi/dS = 0$.

Figure 2 represents a cross section of an infinitely long liquid bar placed on the edge of a half-plane. The profile of this section can be described by $d\phi/dS = cZ$, with the boundary condition $Z = Z_{\max} - Z_0 = \bar{Z}$ at $\phi = 0$ where ϕ is the contact angle. The geometry of the coordinate system gives the auxiliary equation $dZ/d\phi = \sin \phi$. If the value of the characteristic constant, c, is known, the vertical coordinate of the profile can be computed from the equation

$$Z - Z_0$$

$$= - \frac{1}{\sqrt{2c}} \int_{\phi_1}^{\phi} \frac{\sin \phi d\phi}{\sqrt{\cos \phi - \cos \phi_1 + \frac{1}{2c} \left(\frac{d\phi}{dS} \right)_{\phi_1}^2}} \tag{3a}$$

$$= \sqrt{\frac{2}{c}} \left[\sqrt{\cos \phi - \cos \phi_1 + \frac{1}{2c} \left(\frac{d\phi}{dS} \right)_{\phi_1}^2} - \frac{1}{\sqrt{2c}} \left(\frac{d\phi}{dS} \right)_{\phi_1} \right] , \tag{3b}$$

where $(d\phi/dS)_{\phi_1}$ is the curvature at $\phi = \phi_1$ and is determined from

$$\bar{Z} = \sqrt{\frac{2}{c}} \left[\sqrt{1 - \cos \phi_1 + \frac{1}{2c} \left(\frac{d\phi}{dS} \right)_{\phi_1}^2} - \frac{1}{\sqrt{2c}} \left(\frac{d\phi}{dS} \right)_{\phi_1} \right] , \tag{4}$$

where

$$\left(\frac{d\phi}{dS}\right)_{\phi_1} = \frac{1}{Z}[1 - \cos\phi_1] - \frac{c}{2}\,.$$

The area of the cross section is determined from

$$\begin{aligned} A &= 2\int_0^{x_1} (Z - Z_0)dx \\ &= \frac{2}{c}\left[\int_0^{\phi} \frac{d\phi}{dS}\cos\phi dS - \int_0^{x_1}\left(\frac{d\phi}{dS}\right)_{\phi} dx\right] \\ &= \frac{2}{c}\left[\sin\phi_1 - \left(\frac{d\phi}{dS}\right)_{\phi_1} x_1\right]. \end{aligned} \tag{5}$$

When c is unknown, Eqs. (4) and (5) can be combined to eliminate $(d\phi/dS)_{\phi_1}$, and the value of c can be determined by measuring certain dimensions of the profile. This manipulation yields the expression

$$c = \frac{\dfrac{Z}{x_1}\sin\phi_1 + \cos\phi_1 - 1}{\dfrac{Z}{2}\left(\dfrac{A}{x_1} - Z\right)}\,. \tag{6}$$

Table 1 shows values of c computed from Eq. (6) for several different liquids. The horizontal coordinate of the profile can be computed from

$$x = \frac{1}{\sqrt{2c}}\int_0^{\phi} \frac{\cos\phi d\phi}{\sqrt{\cos\phi - \cos\phi_1 + \dfrac{1}{2c}\left(\dfrac{d\phi}{dS}\right)^2_{\phi_1}}}\,. \tag{7}$$

In the case where

$$\frac{1}{2c}\left(\frac{d\phi}{dS}\right)^2_{\phi_1} - \cos\phi_1 > 1 \quad \text{and} \quad \phi \geq 0\,,$$

the solution to Eq. (7) is

$$x = \frac{1}{\sqrt{ck}}\left[(k^2 - 2)u + 2E(u)\right], \tag{8}$$

where $E(u)$ is Legendre's incomplete elliptic integral of the second kind[5] with amplitude u given by

$$\mathrm{am}\,u = \phi/2$$

and

$$k^2 = \frac{2}{1 - \cos\phi_1 + \dfrac{1}{2c}\left(\dfrac{d\phi}{dS}\right)^2_{\phi_1}}\,.$$

In the case where the profile is observed to have the constraints

$$-1 < \frac{1}{2c}\left(\frac{d\phi}{dS}\right)^2_{\phi_1} - \cos\phi_1 \leq 1$$

$$0 \leq \phi < \cos^{-1}\left[\cos\phi_1 - \frac{1}{2c}\left(\frac{d\phi}{dS}\right)^2_{\phi_1}\right]$$

Table 1 Values of c

Material	*c in cm^{-2}*
Water	13.4
Methylene Iodide	64.19
Glycerol	19.5
60-40 Solder	58.01
60-40 Five Core Solder	6.99
Ink A (1419)	12.15
Ink B (D481)	13.86
Ink C (14022)	13.82

Figure 3 Equilibrium forces in solid-liquid-air system.

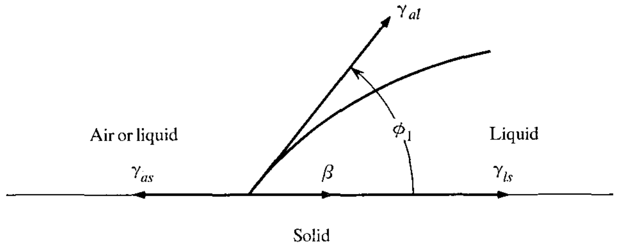

the solution to Eq. (7) is

$$x = \frac{1}{\sqrt{c}}\left[2E(u) - u\right] \tag{9}$$

with

$$\mathrm{am}\,u = \sin^{-1}\left[\frac{1 - \cos\phi}{1 - \cos\phi_1 + \dfrac{1}{2c}\left(\dfrac{d\phi}{dS}\right)^2_{\phi_1}}\right]^{1/2}$$

and

$$k^2 = \frac{1}{2}\left[\frac{1}{2c}\left(\frac{d\phi}{dS}\right)^2_{\phi_1} - \cos\phi_1 + 1\right].$$

The way to use the preceding equations for calculating profiles other than the droplet on a surface will be discussed later.

- *Coefficient of retardation*

The familiar expression, $\gamma_{as} - \gamma_{ls} = \gamma_{al}\cos\phi$, has often been used to define a relationship between the surface tensions that are in equilibrium at the three interfaces separating a solid, a liquid, and a gas, or at the interfaces between a solid and two immiscible liquids, where the forces act parallel to the surface of the solid at the point of intersection (see Fig. 3). (The subscripts in the surface tension terms of the expression have their usual significance for a solid-liquid-air system.) This equation, which according to most investigators was first obtained by Young,[6] implies that there is a unique contact angle, ϕ, for a given solid-liquid-air system in equilibrium. Indeed, Harkins[7] states that any other angle measured is due to improper preparation of the surface and poor measurement techniques. Nevertheless, one can measure not only two distinct contact angles—the maximum advancing contact angle, ϕ_A, and the minimum receding contact angle, ϕ_R—but any angle in between. Coghill and Anderson[8] suggested that hysteresis associated with advancing and receding angles is related to surface roughness. Bartell and Smith[9] further proposed adsorption effects as an explanation for the hysteresis. Pease[10] assumed that for a receding front the determining factor was the work of adhesion of a line passing through the maximum possible number of polar regions; whereas, for an advancing front, the line was through the maximum number of nonpolar regions. Ablett[11] showed that the values of the advancing and receding angles depend on the rate of movement of the three-phase boundary along the solid. Adam and Jessop[12] suggested that hysteresis be formulated in terms of a "frictional force," such that for advancing motion,

$$\gamma_{as} - \gamma_{ls} = \gamma_{al} \cos \phi_A + F ,$$

and that for receding motion,

$$\gamma_{as} - \gamma_{ls} = \gamma_{al} \cos \phi_R - F .$$

To account for the variety of contact angles that can be observed in a system, it was found convenient to define a variable function, β, which incorporates the effects of all fixed parameters, (e.g., surface roughness, viscosity of the liquid, γ_{al}, etc.). Hence, the expression

$$\gamma_{as} - \gamma_{ls} = \gamma_{al} \cos \phi_1 + \beta , \tag{9}$$

implies that there is only one angle for which Young's expression is applicable, and that angle, ϕ_0, is measured when $\beta = 0$.

For any angle ϕ_1 greater than ϕ_0, the value of the β function is given by

$$\beta = \gamma_{al}(\cos \varphi_0 - \cos \phi_1) = \gamma_{al} \sin \phi_1 \frac{\cos \phi_0 - \cos \phi_1}{\sin \phi_1}$$

where $\gamma_{al} \sin \phi_1$ is the force component normal to the solid surface and $(\cos \phi_0 - \cos \phi_1)/\sin \phi_1$ is defined as μ, the coefficient of retardation. As liquid is added to the droplet, the contact angle increases until it reaches a critical value ϕ_A and the base of the droplet spreads. At this point μ reaches a maximum value

$$\mu_{\max A} = \frac{\cos \phi_0 - \cos \phi_A}{\sin \phi_A} , \tag{11}$$

the significance of which is comparable to that of the static coefficient of friction.

When liquid is removed from the droplet, the contact angle decreases until it, also, reaches a critical value, ϕ_R, and the base of the droplet contracts. Here μ takes the value

$$\mu_{\max R} = \frac{\cos \phi_R - \cos \phi_0}{\sin \phi_R} , \tag{12}$$

and if one makes the strong assumption that $\mu_{\max A} = \mu_{\max R}$, the following relation can be derived from Eqs. (11) and (12) to calculate the value of $\mu_{\max}$ for a given liquid-solid-air system:

$$\mu_{\max} = \tan \tfrac{1}{2} (\phi_A - \phi_R) . \tag{13}$$

The point of the preceding explanation is not so much to provide a physical model of the spreading and contracting of a liquid as it is to state that there are two angles ϕ_A and ϕ_R which are characteristic of a given system. Table 2 lists these values for a variety of liquids and the surfaces on which they are deposited. For the designer of liquid junctions these values give the limits on the contact angles that he may wish to specify.

Table 2 Values of advancing and receding contact angles for solid-liquid-gas (or liquid) systems.

Solid	*Liquid*	*Gas or liquid*	ϕ_A	ϕ_R
Cellulose Triacetate	Water	Air	67.5°	52°
Cellulose Triacetate	CH_2I_2	Air	47	39.5
Cellulose Triacetate	C_6H_5Br	Air	7	0
Cellulose Acetobutyrate	Water	Air	75.5	48.5
Cellulose Acetobutyrate	CH_2I_2	Air	43	17
Cellulose Acetobutyrate	C_6H_5Br	Air	14	0
Glass	Water	Oleic Acid	80	55
Wax	Water	Air	133.9	96.20

Figure 4 Sequences of liquid profiles as protrusion is lowered into droplet and withdrawn.

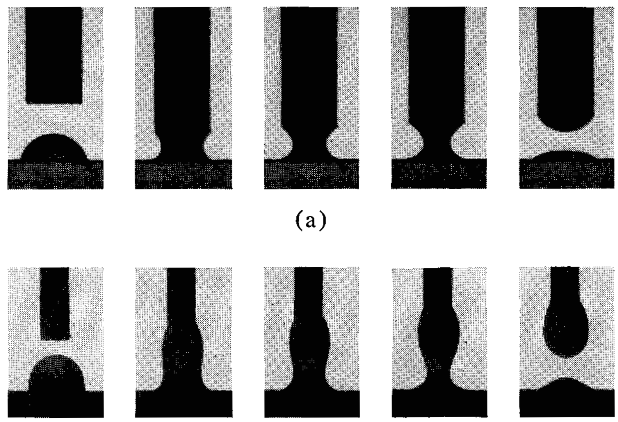

(a)

(b)

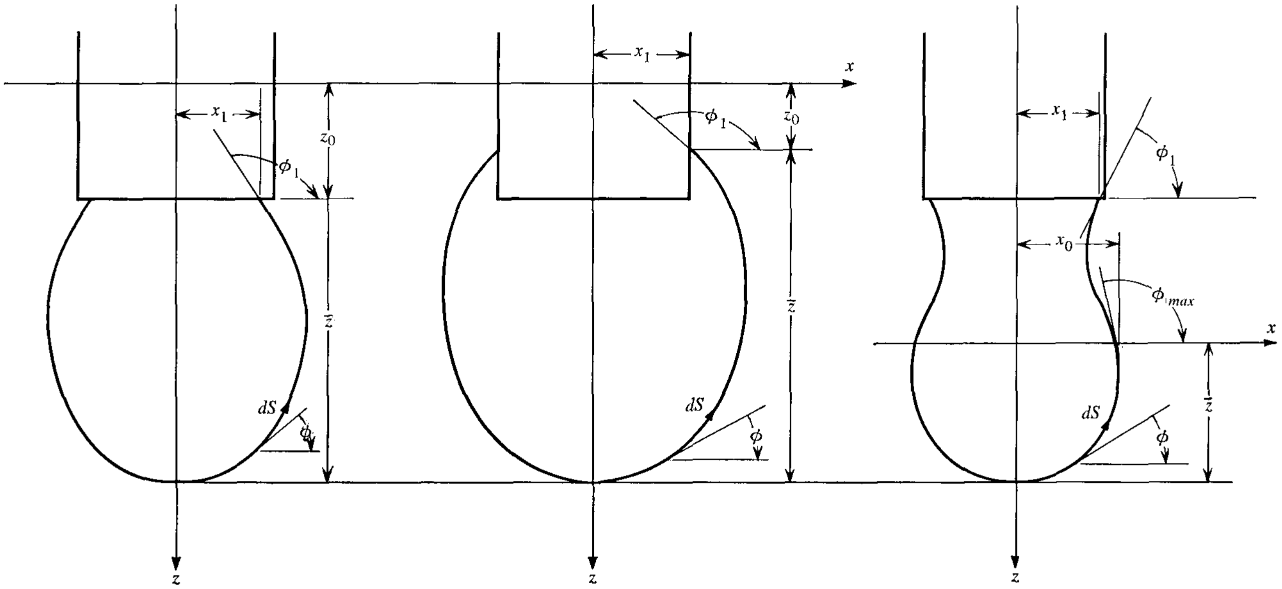

(a) (b) (c)

Figure 5 Droplet hanging from protrusion.

Computation of profiles

In an inking process the liquid profile will take on various shapes as the ink is transferred from the inking surface to the type. Fig. 4 shows two sequences in which a protrusion is lowered toward the inking surface and subsequently raised. In the first sequence the conditions are such that the ink droplet is attached to the bottom of the protrusion, and in the second sequence, the ink droplet is attached to the sides of the protrusion.

The above photographs of the liquid transfer process have demonstrated the conditions that will cause a droplet to "neck" when external tension is applied. For the first sequence, when the liquid is in static equilibrium, (e.g., the second step in the first sequence of Fig. 4), the vertical components of force at the junctions between the liquid and the two surfaces are given by $\gamma_{al} \sin \phi_{\text{top}}$ and $\gamma_{al} \sin \phi_{\text{bot}}$. As external tension is applied to the liquid, the force components will either increase or decrease depending on whether the angles were initially less than or greater than 90°. If the angle is initially less than 90°, as shown in this sequence, the liquid will not separate from the surface as tension increases; rather, as the height of the liquid increases, the width of the "neck" will decrease until the liquid separates into two parts, one on each surface. However, if an angle is initially greater than 90° and the applied external tension reaches a critical value, the liquid will begin to separate from that surface in the normal direction when $\gamma_{al} \sin \phi$ exceeds the adhesive force between the liquid and the surface.

In the second sequence, the ink droplet again "necks" when it is attached both to the bottom surface and the parallel sides of the protrusion. The condition for attachment at the bottom surface in this case is the same as that in the first sequence. On the parallel sides of the protrusion, the liquid will detach from the sides when ϕ_{top} reaches the critical receding contact angle (ϕ_R).

The profiles that occur at the various equilibrium states reached during the transfer process may be computed from the basic equations, (3a) (7), if one makes judicious changes in the variables and boundary conditions. Assuming that the characteristic value, c, has already been found, the profile of the droplet hanging from a protrusion (Fig. 5a) can be calculated simply be turning the picture upside down and using the same variables as before. The fact that the liquid may be attached to the sides as well as to the bottom of the protrusion (Fig. 5b) has no effect on the computation except that the distance Z_0 is measured from the base line to the point on the side of the protrusion where the liquid terminates.

It is also possible to observe a droplet hanging from a protrusion in a stable configuration like that of Fig. 5c. In this case the computation is divided into two parts, the boundary being determined at the point ($Z = 0, x = x_0$) on the profile where the curvature changes from positive to negative or $\phi = \phi_{\max}$. The vertical distance from the bottom of the droplet to this point ($\bar{Z}_0$) and the contact angle ϕ_1 provide the necessary additional boundary conditions.

For the configurations assumed by a droplet suspended between a plane and a protrusion, Fig. 6, the distance $\bar{Z}(\bar{Z}_1$ for Fig. 6c) and angles ϕ_1 and ϕ_2 provide new boundary conditions; otherwise, computation of the profile proceeds as before.

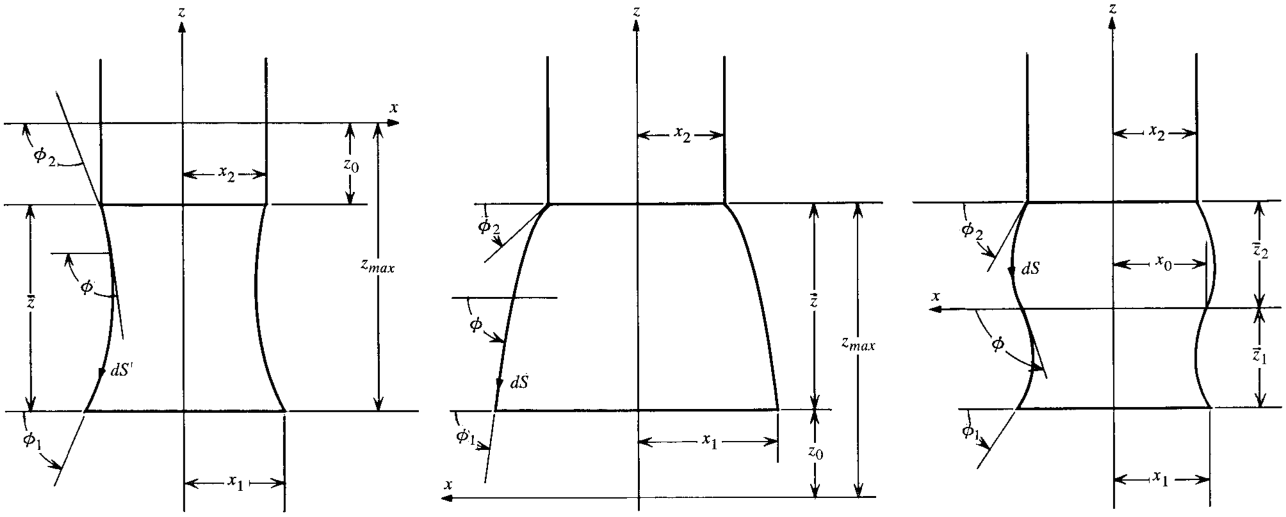

(a) (b) (c)

Figure 6 Droplet suspended between protrusion and plane.

Experimental methods and results

Experiments were devised to test the validity of the theoretical approach. The physical set-up was quite simple and closely followed the geometrical configurations illustrated previously. Three liquids commonly used in contact angle studies were employed: water, glycerine, and methylene iodide. In addition, three different and very viscous proprietary printing inks were used. Two commercially available solders (60-40 five core, and solid 60-40) were investigated in the molten state.

Agreement between the experimentally and theoretically calculated profiles was remarkable, indeed. For convenience, this agreement will be discussed first; then, pertinent experimental methods and procedures will be described. Figures 7a through d show profiles of a droplet of one of the liquids either at rest on a half-plane or suspended between a plane and a protrusion. One-half of each experimental profile was compared with theoretical calculations. The calculated profiles were superimposed on photographs made of the silhouettes of the back-lighted droplets observed in a microscope. Error in the calculations was never more than $\pm 5\%$ with respect to the silhouette measurements.

The long protrusion illustrated in some of the figures was rectangular in cross section. The width of the cross section was smaller than the diameter of the droplet and the length was greater. The photographs were made with the plane of the width at right angles to the camera. The protrusion could be raised and lowered.

The three different liquids and the three different inks were each deposited on a narrow Teflon half-plane with the use of a microburette whose fluid delivery was controlled by a mechanical micrometer. The solders were deposited on a copper half-plane in a different manner. A cylindrical strand of solder (0.044″ dia.) was lowered into contact with a narrow-width copper half-plane maintained at a temperature above the melting point of the solder. The solder strand was withdrawn after a drop of molten solder formed. A tinned copper protrusion, maintained at the identical temperature of the copper half-plane, was then lowered to

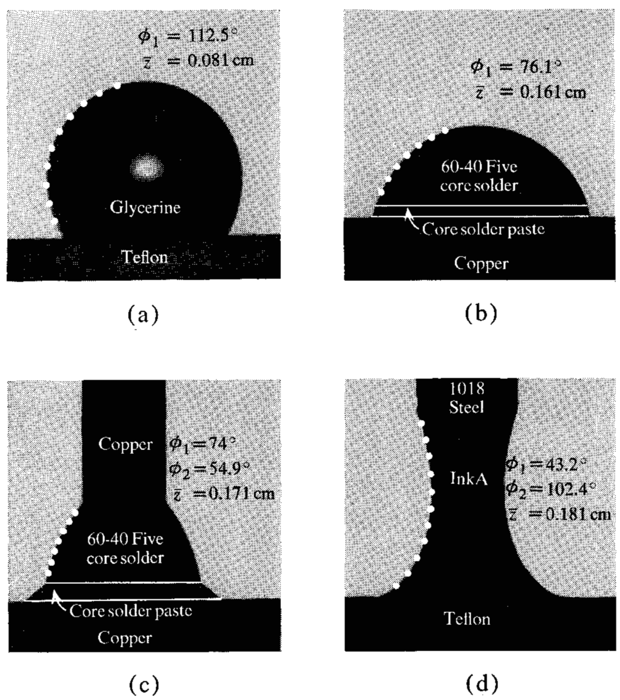

Figure 7 Photographs of liquid profiles with calculated values superimposed.

the exact height of the hemispherical surface of the molten droplet.

The 1018 steel protrusion used with the liquids and the inks was also lowered to the surface of the droplets. All droplets were investigated with the same procedure. The protrusion was slowly raised a few thousandths of an inch and a photograph was made of the silhouette observed in a microscope. The procedure of raising the protrusion and photographing was continued at equal intervals up to the height at which the droplet separated into two parts.

Conclusions

It has been demonstrated that solutions for the Young-Laplace equation can be obtained in closed form for the two dimensional case. There was excellent agreement between calculated and experimental results for various liquids including inks and molten solders. The majority of the solder junctions in practical applications are axially symmetric. The above approach needs to be extended to cover the more general cases.

References

1. A. W. Adamson, *Physical Chemistry of Surfaces*, Interscience Publishers Ltd., 1960, p. 6.
2. F. Bashforth and J. C. Adams, *An Attempt to Test the Theories of Capillary Action*, Cambridge University Press, 1883.
3. J. M. Andreas, E. A. Hauser and W. B. Tucker, *J. Phys. Chem.* **42,** 1001 (1938).
4. L. S. Goldmann, private communication.
5. P. F. Birds and M. D. Freidman, *Handbook of Elliptic Integrals for Engineers and Physicists*, Springer-Verlag, 1954, p. 8.
6. T. Young, *Phil. Trans. Roy. Soc. London* **94,** 65 (1805).
7. W. D. Harkins, *The Physical Chemistry of Surface Films*, Reinhold Publishing Corp., 1952, p. 280.
8. W. H. Coghill and C. O. Anderson, *U. S. Bur. Mines Tech. Papers* **262,** 54 (1924).
9. F. E. Bartell and J. T. Smith, *J. Phys. Chem.* **57,** 165 (1953).
10. D. C. Pease, *J. Phys. Chem.* **49,** 107 (1945).
11. R. Ablett, *Phil. Mag.* **6,** 46, 244 (1923).
12. N. K. Adam and G. Jessop, *J. Chem. Soc.* 1863 (1925).

Received January 15, 1968.